Relationship between wind speed and gas exchange over the ocean revisited

Rik Wanninkhof
Atlantic Oceanographic and Meteorological Laboratory (AOML) of NOAA, 4301 Rickenbacker Causeway, Miami, FL 33149

Abstract

The relationship between gas exchange and wind speed is used extensively for estimating bulk fluxes of atmospheric gases across the air-sea interface. Here, I provide an update on the frequently used method of Wanninkhof (1992). The update of the methodology reflects advances that have occurred over the past two decades in quantifying the input parameters. The general principle of obtaining a relationship constrained by the globally integrated bomb-$^{14}CO_2$ flux into the ocean remains unchanged. The improved relationship is created using revised global ocean ^{14}C inventories and improved wind speed products. Empirical relationships of the Schmidt number, which are necessary to determine the fluxes, are extended to 40°C to facilitate their use in the models. The focus is on the gas exchange of carbon dioxide, but the suggested functionality can be extended to other gases at intermediate winds ($\approx$4-15 m s^{-1}). The updated relationship, expressed as k = 0.251 $\langle U^2 \rangle$ (Sc/660)$^{-0.5}$ where k is the gas transfer velocity, $\langle U^2 \rangle$ is the average squared wind speed, and Sc is the Schmidt number, has a 20% uncertainty. The relationship is in close agreement with recent parameterizations based on results from gas exchange process studies over the ocean.

Determining fluxes of gases between the ocean and atmosphere is critical for several biogeochemical cycles, most notably the carbon cycle. Air-sea fluxes of carbon dioxide are commonly determined by measuring partial pressure gradients between the surface ocean and lower atmosphere and then multiplying them by a parameter called the gas transfer velocity. The approach used to determine regional-to-global fluxes from surface water concentrations has remained unchanged, but input parameters are now better constrained.

Air-sea gas fluxes at regional-to-global scales are generally determined using a bulk flux equation:

$$F = k (C_w - C_a) \qquad (1)$$

where F is the flux (mass area^{-1} time^{-1}), k is the gas transfer velocity (length time^{-1}), and C_w and C_a are the concentrations (mass volume^{-1}) in the bulk liquid and at the top of the liquid boundary layer adjacent to the atmosphere. Concentration gradients are determined by measuring them in observational campaigns and then extrapolating their values in time and space (Takahashi et al. 2009), using field data and parameteri-

zations based on other surface water properties (Telszewski et al. 2009; Sasse et al. 2013), or by obtaining them from general circulation ocean biogeochemical models (see, e.g., Doney et al. 2009). For sea-air CO_2 fluxes, the bulk equation is frequently expressed in terms of partial pressure:

$$F = k K_0 (pCO_{2w} - pCO_{2a}) \qquad (2)$$

where K_0 is the solubility (mass volume^{-1} pressure^{-1}), and pCO_{2w} and pCO_{2a} (pressure) are the partial pressures of CO_2 in equilibrium with surface water and in the above lying air, respectively. Partial pressure is sometimes expressed as a fugacity that takes into account the non-ideal behavior of CO_2 gas (Weiss 1974). The partial pressure difference, $pCO_{2w} - pCO_{2a}$, or ΔpCO_2, and fugacity difference, ΔfCO_2, have virtually the same numeric value.

The gas transfer velocity is frequently parameterized as a function of wind speed. Wind does not directly control gas transfer; rather, gas transfer is governed by complex boundary layer processes. However, most of these boundary layer processes are strongly influenced by wind and, on a global scale, wind can be used as the sole environmental forcing. The relationship of gas transfer with wind is frequently expressed as a quadratic dependency (Broecker et al. 1986; Wanninkhof 1992; Sweeney et al. 2007), and results from laboratory and field studies with gases of low solubility can be well represented by such a dependency (Ho et al. 2011). Theoretical con-

siderations where gas transfer is modeled as a function of wind stress support a quadratic dependence. However, there are both observational and theoretical results suggesting that different functionalities would be more appropriate under certain conditions and specific environments (Fairall et al. 2000) and on global scales (Krakauer et al. 2006).

The relationship of gas transfer and wind implicitly assumes that the wind "grips" the water surface and induces turbulence and shear in the liquid boundary layer ($\approx$100 micron thickness) that controls the transfer of gases with low solubility. A key parameter for expressing the impact of wind on the ocean surface is friction velocity, as friction velocity is a parameter directly related to the mass boundary layer of the water. Many dedicated gas transfer studies in the laboratory and field have provided friction velocities, but global forcing fields are mostly expressed as wind speed at the 10 m height. The conversion from wind speed to friction velocity requires knowledge of the air boundary layer stability, the direction of winds relative to waves and swell, surfactant levels, and the magnitude and direction of surface ocean currents.

For regional to global flux estimates, remotely sensed winds from scatterometers or passive microwave sensors on satellites are used extensively. In these cases, the winds derived from microwave signals returned from the water surface are directly related to wind stress (Risien and Chelton 2008). The variability of stress and neutral winds at the 10-m height derived from the remote sensing signals is very similar because the marine atmosphere has near neutral stratification, and the magnitude of ocean currents is small relative to wind speed for most ocean areas (Liu et al. 2008). The wind speeds reported in remote sensing products as used here are equivalent winds at 10-m height under neutral boundary conditions, U_{10n}.

The magnitude of gas transfer will differ with different wind and turbulence regimes. At low winds with smooth water surfaces (with winds less than about 3 m s^{-1}), factors such as chemical enhancement and thermal gradients affect the exchange to a greater extent than wind such that the gas transfer velocity is not, or only weakly, dependent on wind (Wanninkhof and Knox 1996; McGillis et al. 2004; Zappa et al. 2007). At high winds ($\approx$>15 m s^{-1}), bubble entrainment becomes a major factor in gas transfer (Monahan and Dam 2001; McNeil and D'Asaro 2007). There is considerable amount of uncertainty in the high wind speed regime because of unresolved questions of gas transfer through bubbles and the turbulence structures under these conditions. Gas transfer at high winds can be parameterized as a function of whitecap coverage (Asher et al. 1996) that, in turn, relates to wind by a cubic or higher dependency (Monahan and Spillane 1984). The transfer processes through bubbles are gas specific and depend on the chemical and physical properties of the gas. A cubic dependence with wind is in accord with energy dissipation theories of boundary layer turbulence.

The recognition of three distinct turbulence environments, as reflected by the wave state, has provided the basis for a seg-

mented gas exchange-wind speed relationship, with a smooth boundary regime at low winds, a regime with capillary and gravity waves at intermediate winds, and a regime with wave breaking at high winds (Liss and Merlivat 1986). An adaptation of this idea is that several of the processes described could control gas transfer proportionally to wind, which has led to the development of hybrid models where the gas exchange–wind speed relationship is expressed as a third-order polynomial function (Woolf 2006; Wanninkhof et al. 2009). However, as shown by Wanninkhof et al. (2009), this functionality can be well approximated by a quadratic fit in the wind speed range of 3-15 m s^{-1}. Winds greater than 15 m s^{-1} occur 3% to 6% of the time (Fig. 1) and, whereas these high winds are disproportionately important for fluxes of low solubility climate-relevant gases, a single quadratic fit can be used for basin-to-global scale estimates.

Parameterizations using other inputs and incorporating boundary layer physics have been created (Fairall et al. 2000; Jackson et al. 2012; Glover et al. 2002; Erickson 1993) but are generally complex, and uncertainty in the input parameters and physical models underlying the relationships has limited their use. Quadratic relationships have been developed based on several field studies, and strong agreement is noted between field studies in a number of environments (Nightin-
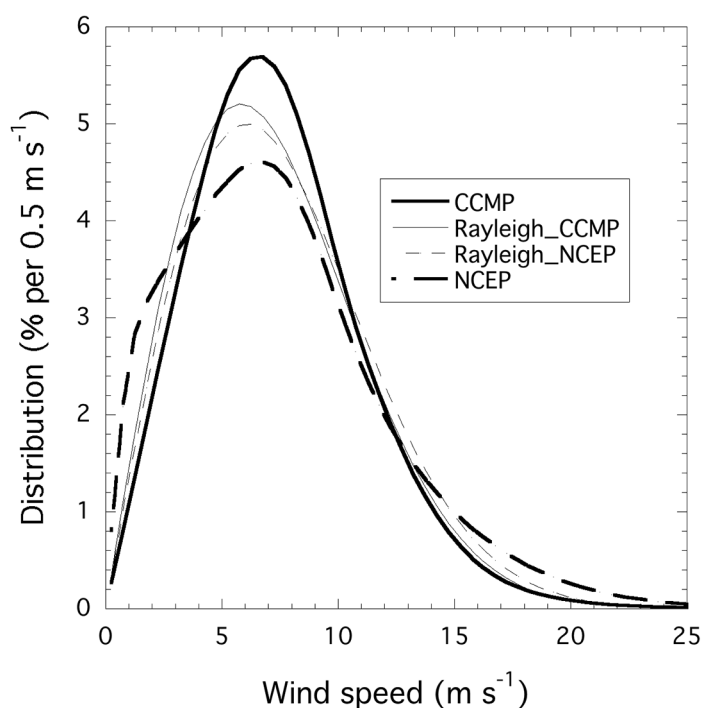
Fig. 1. Histogram of the distribution of winds over the ocean for 1990-2009. The Cross Calibrated Multi-Platform (CCMP) wind product (solid line) (Atlas et al. 2011) is used to develop the proposed relationship, k_{660} = 0.251 × U_{10}^2. The NCEP-2 product (thick dashed line) has been used in other global flux estimates. The thin solid and dashed lines are the Rayleigh distributions for a global mean wind of 7.3 m s^{-1} (CCMP) and 7.6 m s^{-1} (NCEP-2), respectively.

gale et al. 2000; Ho et al. 2006).

A strong functionality of gas transfer with wind has been observed in dedicated field studies and wind wave tanks. Global and regional mass balance approaches have not provided strong evidence of such dependencies (Smethie et al. 1985; Krakauer et al. 2006). Krakauer et al. (2006) used regional ^{13}C and ^{14}C isotopic information and wind speeds with a minimum misfit approach and obtained a square root dependence with wind (0.5 ± 0.4) that is significantly less than 2 for the quadratic used here. It is possible that errors in the ocean transport models or monthly averaged winds used causes the weak dependency.

The relationship of gas exchange with wind speed proposed by Wanninkhof (1992) (W-92) was based on several assumptions and input parameters. Knowledge of these input parameters and constraints has improved over the past two decades, providing a strong rationale for an update. In short, in W-92, a quadratic dependence of gas exchange with wind speed was assumed for the open ocean based on wind-wave tank studies (Liss 1973; Wanninkhof and Bliven 1991). A global mean wind speed, U_{av} of 7.4 m s^{-1} was used (Wentz et al. 1984), along with a globally averaged gas transfer velocity of 22 cm h^{-1}, from which a global parameterization of $k_{av} = 0.39\ U_{av}^2$ (Sc/660)$^{-0.5}$ was obtained, where Sc was the Schmidt number. This relationship was valid for long-term averaged winds of a year or more. To estimate a relationship for instantaneous (short-term) winds, a Rayleigh distribution for global winds was assumed from which the relationship $k = 0.31\ U_{10}^2$ (Sc/660)$^{-0.5}$ was derived.

Methods

This update involves improvements in the basic assumptions and constraints that went into the W-92 relationship. A reassessment of the amount of bomb-^{14}C in the ocean yields a lower inventory and leads to a lower globally averaged gas transfer velocity (Naegler et al. 2006; Sweeney et al. 2007; Graven et al. 2012). Large improvements in determining wind speeds over the ocean, particularly using remote sensing, have led to a more accurate representation of the winds (Atlas et al. 2011). The better estimates of winds and bomb-^{14}C inventory are used in a global ocean inverse model whose gas exchange parameterization is optimized to reach consistent results between the atmospheric ^{14}C trend and the oceanic ^{14}C inventory (Sweeney et al. 2007). A cost function is used to optimize the coefficient of gas transfer:

$$a = k\ \langle U^2 \rangle^{-1}\ (Sc/660)^{-0.5} \qquad (3)$$

where $\langle U^2 \rangle$ denotes the average of neutral stability winds at 10-m height (U_{10n}) squared, or the second moment.

Bomb-^{14}C estimate

The ^{14}C released during aboveground thermonuclear bomb testing in the 1960s increased the ^{14}C levels in the atmosphere by almost a factor of 2, and the addition is referred to as bomb-^{14}C. This perturbation can be used as a global gas transfer experiment in that the bomb-^{14}C is taken up by the ocean through gas exchange. By monitoring the inventory of bomb-^{14}C in the ocean and the changes in atmospheric ^{14}C levels, and by accounting for the pre-bomb-^{14}C content in these reservoirs, gas transfer can be determined. Initial estimates of ocean bomb-^{14}C inventories were performed in a fairly simplistic manner with limited data and yielded a value of 289×10^{26} atoms bomb-^{14}C for the mid-1970s (Broecker et al. 1985). Since these initial estimates, several improvements have been made in both the separation of natural ^{14}C from bomb-^{14}C and the spatial distribution of ^{14}C (Rubin and Key 2002). Using these improved methodologies, lower inventories of 259-265 $\times 10^{26}$ and 320-350 $\times 10^{26}$ atoms bomb-^{14}C in the ocean were derived for the mid-1970s and mid-1990s, respectively (Peacock 2004). With this improved, spatially resolved ^{14}C dataset, inverse techniques using global ocean circulation models were applied to optimize the gas transfer. Naegler (2009) accounted for the flux of ^{14}C out of the oceans to further refine the ^{14}C gas exchange estimate.

Wind speed product

Several wind speed products are available that provide global coverage, but they have appreciable differences (Wallcraft et al. 2009). The Cross-Calibrated Multi-Platform (CCMP) product at 0.25° and 6-h resolution is chosen for determining the gas exchange wind speed relationship. The high-resolution product captures the full variability over the ocean, and the product is data constrained because of the multiple remote sensors used. It is well documented (Atlas et al. 2011; Hoffman et al. 2013), and data are readily accessible (http://podaac.jpl.nasa.gov/datasetlist?search = ccmp). As can be inferred from Eq. 3, the "a" coefficient determined from the inverse method will depend on the magnitude of the wind. In other words, depending upon which wind product is used, the coefficient will differ. By determining the optimal "a" coefficient for the appropriate winds, uncertainty in the global fluxes can be decreased. The high temporal and spatial resolution of the wind product also eliminates the need to cope with the impact of nonlinearity on the relationship, as is the case when using averaged winds (Wanninkhof et al. 2002).

Optimal coefficient

The optimization of the coefficient (Eq. 3) depends on the distribution of ^{14}C in the ocean, the wind speed product, and the method used to determine the coefficient. The optimal coefficient obtained from using an inverse modeling approach, the CCMP winds, and the Modular Ocean Model-General Circulation Model, MOM3 GCM, as described in Sweeney et al. (2007), yields a coefficient of 0.251, thereby providing the updated gas exchange wind speed relationship:

$$k = 0.251\ \langle U^2 \rangle\ (Sc/660)^{-0.5} \qquad (4)$$

where, by convention, the units of k are in cm h^{-1} and U is in m s^{-1}. Thus, the units of the coefficient 0.251 are (cm h^{-1}) (m

$s^{-1})^{-2}$. The uncertainty estimate of k for global or basin-scale applications is 20% as detailed below. This is appreciably smaller than the uncertainty quoted in Sweeney et al. (2007) of ≈30%. The smaller uncertainty takes into account that the product of coefficient, a, and wind speed are constrained by the global value of k (see e.g., Neagler 2009) and a downward revision of the uncertainty in bomb ^{14}C estimate in the ocean (Sweeney pers. comm.). There is good correspondence of gas exchange wind speed relationships obtained in several ocean gas exchange studies with the equation above (Ho et al. 2011; Nightingale et al. 2000).

The gas transfer velocity is a function of temperature through its Schmidt number dependency. Fig. 2 shows the effect of temperature on k by providing the k of CO_2 at 0, 20, and 40°C. Other gas exchange-wind speed relationships that have appeared in the literature are shown as well in the figure. However, interpretation of the good correspondence must be done with caution as other methods and wind speed products are used to create these relationships.

By combining Eqs. 2 and 4, the bulk flux can be expressed as:

$$F = 0.251 <U^2> (Sc/660)^{-0.5} K_0 (pCO_{2w} - pCO_{2a}) \qquad (5)$$

In the case of the air-sea CO_2 flux determination, a simplifying assumption can be made with a small increase in uncertainty. The approximation is that the product, $(Sc/660)^{-0.5} K_0$, is almost invariant with temperature (Etcheto and Merlivat 1988). The CO_2 fluxes can then be directly determined according to

$$F = 7.7 \times 10^{-4} <U^2> \Delta pCO_2 \qquad (6)$$

where F has the units of mol m^{-2} y^{-1}, $<U^2>$ is in $(m\ s^{-1})^2$, and ΔpCO_2 is in μatm. The global CO_2 flux using Eq. 6 is 1% greater than using the exact expression (Eq. 5) as applied to the Takahashi ΔpCO_2 climatology (Takahashi et al. 2009). Local differences between the exact equation and the approximation at high and low temperatures can reach 5%.

Schmidt numbers and solubilities

The Schmidt number is defined as the kinematic viscosity of the water divided by the diffusion coefficient of the gas. It is a critical parameter for determining the gas transfer velocity of a gas and for relating the gas transfer velocities of different gases. The Schmidt number is gas- and temperature-specific, and, to a lesser extent, dependent on the salinity of the water. The Schmidt number dependency offers the means to determine the gas transfer velocity for any slightly soluble gas over a range of temperatures with the caveats mentioned below. It is a calculated parameter derived from measurements or empirical estimates of the viscosity of water and diffusion coefficients of the gases in question.

In W-92, the Schmidt number for a range of slightly soluble gases was fit with a third-order polynomial from 0-30°C.
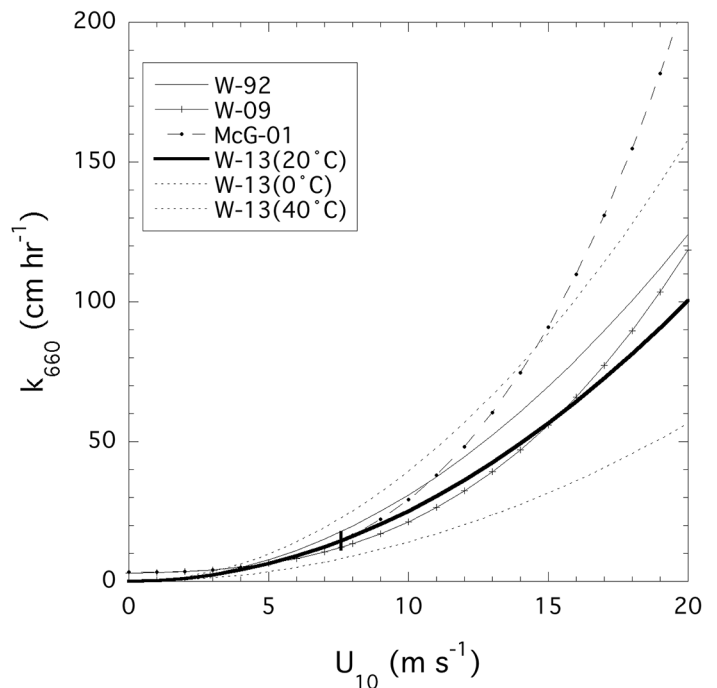
Fig. 2. Relationships between gas transfer velocities and wind speed. The gas transfer velocities are for seawater at 20°C (Sc = 660) unless otherwise noted. The thin solid line (W-92) is that of Wanninkhof (1992). The line with plus symbols (W-09) is the hybrid model proposed in Wanninkhof et al. (2009). The thin dashed line with small solid circles is the cubic relationship of McGillis et al. (2001). The thick solid line (W-13) is the relationship presented here with the stippled lines showing the relationship at 40°C (top) and 0°C (bottom.). The vertical line at the mean global wind of 7.3 m s^{-1} depicts the 20% uncertainty in the relationship. The relationships proposed in Ho et al. (2011), Sweeney et al. (2007), and Nightingale et al. (2000) are similar to the W-13 relationship.

However, water temperatures in extreme environments exceed this range. In prognostic ocean models, sea surface temperatures will exceed 30°C in future climate scenarios. Because polynomials are ill-behaved beyond the range of fit, a refit is provided in Table 1 for temperatures from –2 to 40°C. To avoid systematic errors in the fit over the larger temperature range, a fourth-order fit was applied rather than a third-order fit.

The kinematic viscosities of water and seawater were obtained from a review of the thermo-physical properties of seawater (Sharqawy et al. 2010). Diffusion coefficients are either from laboratory measurements or from fits based on temperature, the dynamic viscosity of water, n_B, and the molar volume of gas at boiling point, V_a, as proposed in Wilke and Chang (1955) with the revised association factor of water provided in Hayduk and Laudie (1974).

$$D = 4.72 \times 10^{-7} T (n_B V_a)^{0.6})^{-1} \qquad (7)$$

Diffusion coefficients of several additional gases have been measured since W-92 and added to the summary. These results

Table 1. Coefficients for a least squares fourth-order polynomial fit of Schmidt number versus temperature for seawater (35‰) at temperatures from –2°C to 40°C.

Gas	A	B	C	D	E	Sc (20°C)
Seawater						
^{3}He	369.11	–19.485	0.60131	–0.011005	0.000087258	146
He	416.36	–21.979	0.67828	–0.012413	0.000098427	165
Ne	844.95	–48.305	1.5615	–0.029273	0.00023487	307
Ar	2078.1	–146.74	5.6403	–0.11838	0.0010148	615
O_2	1920.4	–135.6	5.2122	–0.10939	0.00093777	568
N_2	2304.8	–162.75	6.2557	–0.13129	0.0011255	682
Kr	2252	–147.33	5.1729	–0.10141	0.00083242	696
Xe	2975.2	–201.06	7.2057	–0.14287	0.0011798	882
CH_4	2101.2	–131.54	4.4931	–0.08676	0.00070663	687
CO_2	2116.8	–136.25	4.7353	–0.092307	0.0007555	668
N_2O	2356.2	–166.38	6.3952	–0.13422	0.0011506	697
Rn	3489.6	–244.56	8.9713	–0.18022	0.0014985	985
SF_6	3177.5	–200.57	6.8865	–0.13335	0.0010877	1028
DMS	2855.7	–177.63	6.0438	–0.11645	0.00094743	941
CFC-12	3828.1	–249.86	8.7603	–0.1716	0.001408	1188
CFC-11	3579.2	–222.63	7.5749	–0.14595	0.0011874	1179
CH_3Br	2181.8	–138.4	4.7663	–0.092448	0.0007547	701
CCl_4	4398.7	–308.25	11.798	–0.24709	0.0021159	1315
Fresh water						
^{3}He	335.69	–17.776	0.55017	–0.010087	0.000080066	132
He	378.65	–20.051	0.62059	–0.011378	0.000090314	149
Ne	767.81	–44.402	1.4465	–0.027238	0.00021905	276
Ar	1888.4	–134.55	5.2003	–0.10946	0.00093975	552
O_2	1745.1	–124.34	4.8055	–0.10115	0.00086842	510
N_2	2094.4	–149.23	5.7676	–0.1214	0.0010423	612
Kr	2046.4	–135.21	4.7805	–0.094097	0.00077413	625
Xe	2703.6	–184.46	6.6553	–0.13249	0.0010964	792
CH_4	1909.4	–120.78	4.1555	–0.080578	0.00065777	617
CO_2	1923.6	–125.06	4.3773	–0.085681	0.00070284	600
N_2O	2141.2	–152.56	5.8963	–0.12411	0.0010655	626
Rn	3171	–224.28	8.2809	–0.16699	0.0013915	884
SF_6	3035	–196.35	6.851	–0.13387	0.0010972	953
DMS	2595	–163.12	5.5902	–0.10817	0.00088204	844
CFC-12	3478.6	–229.32	8.0961	–0.15923	0.0013095	1066
CFC-11	3460	–217.49	7.4537	–0.14423	0.0011761	1126
CH_3Br	2109.2	–135.17	4.6884	–0.091317	0.00074715	670
CCl_4	3997.2	–282.69	10.88	–0.22855	0.0019605	1181

Sc = A + Bt + Ct^2 + dt^3 + Et^4 (t in °C). The last column is the calculated Schmidt number for 20°C. The Schmidt number is the kinematic viscosity of water divided by the molecular diffusion coefficient of the gas. The kinematic viscosity for fresh water and seawater are from Sharqawy et al. (2010). The diffusion coefficients of gases are from the following: ^{3}He, He, Ne, Kr, Xe, CH_4, CO_2, and Rn measured by Jähne et al. (1987); Ar, O_2, N_2, N_2O, and CCl_4 fit using Wilke and Chang (1955) as adapted by Hayduk and Laudie (1974); SF_6 measured by King and Saltzman (1995); DMS measured by Saltzman et al. (1993); CFC-11 and CFC-12 measured by Zheng et al. (1998); CH_3Br measured by De Bruyn and Saltzman (1997a).

are generally parameterized with temperature according to

$$D = A\, e^{-E_a/RT} \tag{8}$$

where A is a gas specific constant of proportionality, E_a is a gas specific activation energy of diffusion, R is the ideal gas con-

stant, and T is the absolute temperature. Table 1 includes footnotes that indicate which diffusion coefficients were measured and fit according to Eq. 8 and which diffusion coefficient were estimated from Eq. 7.

The effect of salinity on kinematic viscosity is well determined and parameterized. However, the salinity effect on the

diffusion coefficient of gases is not well known. Jähne et al. (1987) determined experimentally that the diffusion coefficient for He in seawater was 6% less than for fresh water. However, King and Saltzman (1995), De Bruyn and Saltzman (1997a), and Zheng et al. (1998) did not observe an appreciable difference in diffusion coefficients using fresh water or a 35 g/L sodium chloride (NaCl) solution for sulfur hexafluoride (SF_6), methyl chloride (CH_3Cl), and trichlorofluoromethane (CFC-11), respectively. They did, however, measure lower diffusion coefficients for salt water compared with fresh water ranging from 4% to 7% for methane (CH_4) and difluorodichloromethane (CFC-12). Whenever available, the measured diffusivities of gases in seawater were fit to Eq. 8; in all other entries in Table 1, a 6% smaller diffusion coefficient was assumed for seawater ($S \approx 35$) than for fresh water.

The uncertainty in measured and calculated diffusion coefficients is approximately 5% (Jähne et al. 1987) such that the square root Schmidt number dependency in Eq. 4 has a 3% uncertainty assuming no uncertainty in the kinematic viscosity. The different curve-fitting routines and different kinematic viscosities between W-92 and this work have less than a 2% impact on the calculated Schmidt numbers for CO_2 for the common temperature range (Fig. 3). The difference in the Schmidt numbers of SF_6, CFC-11, and CFC-12 based on the recently measured diffusion coefficients compared with the values estimated in W-92 is appreciable, as shown in Fig. 3.

Solubility values as a function of temperature and salinity are provided in Table 2. The values are obtained from the literature with the citations provided. The temperature and salinity dependence of most gases are expressed in terms of an integrated van't Hoff equation including a logarithmic Setchenow salting out dependence as further detailed in papers by Weiss and coauthors (see e.g., Weiss 1974). Solubilities are either expressed as dimensionless ratios of concentration at 0°C (Bunsen coefficient), or in terms of the ratio of liquid phase concentration and gas phase fugacity (mol L^{-1} atm^{-1}). The nomenclature is often inconsistent and expressions and units differ. Table 2 provides the expressions and units as provided by the authors. The approximate conversions are provided in the legend. Summaries of aqueous solubility measurements are also available from Wilhelm et al. (1977), and more recently, in a numerical recipes paper on air-sea gas transfer from Johnson (2010).

Assessment

Here I focus on the differences in the presented gas exchange-wind speed relationship to that of W-92 and the uncertainty in the gas transfer velocity when applied to determine global air-sea CO_2 fluxes. The quadratic functionality and the principles for developing the relationship remain the same. The overall constraint for the gas transfer velocity is the bomb-^{14}C inventory. This inventory estimate has improved by inclusion of more data, a better separation of the bomb-^{14}C and natural ^{14}C, and improved interpolation techniques. The
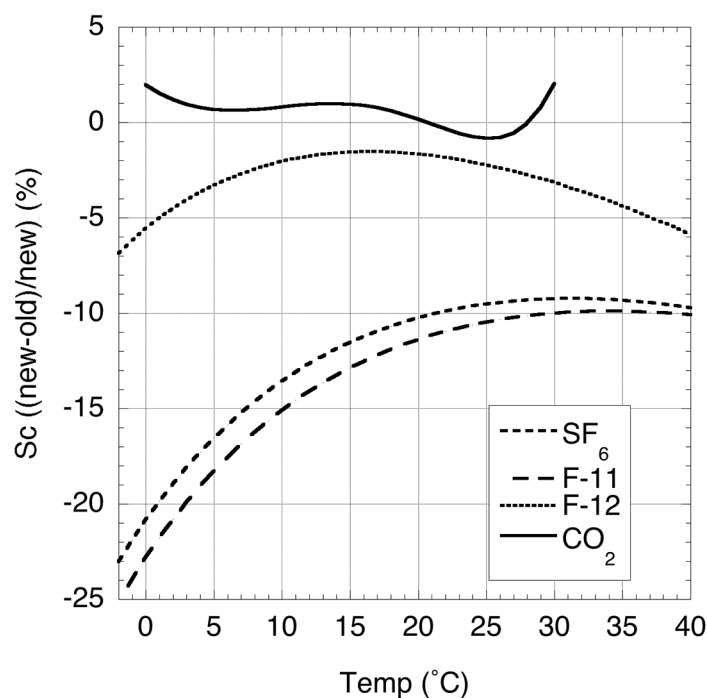
Fig. 3. Differences of Schmidt numbers for CO_2, SF_6, CFC-11, and CFC-12 between the values presented in Table A1 of W-92 and the estimates based on the coefficients shown in Table 1. For CO_2, the differences are due to small differences in kinematic viscosity and curve fitting. For SF_6, CFC-11, and CFC-12, the differences are due to the use of measured diffusion coefficients that were not available in W-92.

bomb-^{14}C inventory for 1995 of 343×10^{26} atoms ^{14}C is used (Sweeney et al. 2007).

In W-92 the global averaged transfer velocity, k_{av}, was determined from the best bomb-^{14}C inventory available at the time of 289×10^{26} atoms bomb-^{14}C for the mid-1970s, yielding a k_{av} of 22 cm h^{-1}. The revised estimate of k_{av} of 17 cm h^{-1} shows a larger decrease than the downward revision of bomb-^{14}C of $\approx 260 \times 10^{26}$ atoms due to improved spatial information of bomb-^{14}C in the ocean (Naegler et al. 2006; Naegler 2009). In the original relationship, this k_{av} was used with the globally averaged wind speed, U_{av}, to derive a relationship between long-term U_{av} and k_{av}. A global wind speed pattern following a Rayleigh distribution was then used to estimate a "short-term" relationship between k and U. Both the magnitude of global wind speed and its distribution were uncertain due to limited data. Greatly improved wind speed coverage from satellites now provides global wind products with high spatial and temporal resolution. In the updated estimate, an inverse model using 6-h CCMP winds was applied to determine the relationship between k and U, thereby avoiding the uncertainties and biases from invoking a universal wind speed distribution. The inverse model and procedures are the same as in Sweeney et al. (2007) except that the CCMP winds rather than the NCEP1 wind product is used, and a correction is applied for bomb [14]C

Table 2. Coefficients for temperature and salinity dependence of solubilities of selected gases.

	A_1	A_2	A_3	B_1	B_2	B_3	Ref
He	−34.6261	43.0285	14.1391	−0.042340	0.022624	−0.0033120	A
^{3}He	(see * below)						
Ne	−39.1971	51.8013	15.7699	−0.124695	0.078374	−0.0127972	A
Ar	−55.6578	82.0262	22.5929	−0.036267	0.016241	−0.0020114	B
O_2	−58.3877	85.8079	23.8439	−0.034892	0.015568	−0.0019387	B
N_2	−59.6274	85.7661	24.3696	−0.051580	0.026329	−0.0037252	B
Kr	−57.2596	87.4242	22.9332	−0.008723	−0.002793	0.0012398	C
Xe	−7.48588	5.08763	4.22078	−0.00817791	−0.0120172		D
CH_4	−68.8862	101.4956	28.7314	−0.076146	0.043970	−0.006872	E
CO_2	−58.0931	90.5069	22.2940	0.027766	−0.025888	0.0050578	F
N_2O	−62.7062	97.3066	24.1406	−0.058420	0.033193	−0.0051313	G
Rn	−76.14	120.36	31.26	−0.2631	0.1673	−0.0270	H
SF_6	−96.5975	139.883	37.8193	0.0310693	−0.0356385	0.00743254	I
DMS	−12.64	35.47					J
CFC-12	−122.3246	182.5306	50.5898	−0.145633	0.092509	−0.0156627	K
CFC-11	−134.1536	203.2156	56.2320	−0.144449	0.092952	−0.0159977	K
CH_3Br	−171.2	254.3	77.04	−0.1828	0.03142		L
CCl_4	−166.321	252.542	71.5211	−0.41216	0.273093	−0.0460112	M

The solubility is expressed as $\ln \beta = A_1 + A_2 (100/T) + A_3 \ln (T/100) + S [(B_1 + B_2(T/100) + B3 (T/100)^2]$ where β is the dimensionless Bunsen coefficient, or K' or K_0, the solubility expressed in mol L⁻¹ atm⁻¹ as noted below. T is in Kelvin and S in ‰. K' and K_0 are expressed in mol L⁻¹ atm⁻¹ where K_0 is for dry gas and K' is for water saturated gas. $K' \approx K_0 f/(X [P − P_{H2O}])$ where f is the fugacity, X is mole fraction (dry), P is total pressure, and P_{H2O} is the water vapor pressure. The reader should consult and reference the original citations for the subtleties of the measurements, units, and the uncertainties in the fits.

*Bunsen coefficient, β: $\beta_{3He} = \beta_{4He}$ (0.9884 − 1.1 × 10⁻⁴ t), t in °C (Weiss (1970a)

A: β, Weiss (1971); B: β, Weiss (1970b); C: β, Weiss and Kyser (1978); D: Fit of data of Wood and Caputi (1966) by Roberta C. Hamme (University of Victoria). Saturation concentration μmol kg⁻¹ atm⁻¹ for moist air see: http://web.uvic.ca/ ~rhamme/Xesol.m $\ln[Xe] = (A_1 + A_2 Ts + A_3 Ts^2) + S (B_1 + B_2 Ts))$, $Ts = \ln([571.3 − T]/T)$; E: β, Wiesenburg, and Guinasso (1979); F: K', (mol L⁻¹ atm⁻¹) Weiss (1974); G: K', (mol L⁻¹ atm⁻¹) Weiss and Price (1980) H: β, Schubert et al. (2012); I: K', (mol L⁻¹ atm⁻¹) Bullister et al. (2002); J: K_0, (mol L⁻¹ atm⁻¹) Dacey et al. (1984); K: K' (mol L⁻¹ atm⁻¹) Warner and Weiss (1985); L: K_0, (mol L⁻¹ atm⁻¹) De Bruyn and Saltzman (1997b); M: K', (mol L⁻¹ atm⁻¹) Bullister and Wisegarver (1998)

evasion from the ocean as detailed in Naegler (2009). For comparison, the global wind speed used in W-92 was 7.4 m s⁻¹ whereas the 20-year CCMP averaged wind speed (1990-2009) is 7.3 m s⁻¹, which is very similar. However, global average winds from different wind speed products range from 6.6 to 7.9 m s⁻¹ (Naegler et al. 2006) and will yield a 40% range in the coefficient, even with the same ¹⁴C constraints. This emphasizes the point that the magnitude of the coefficient is uniquely tied to the wind product used.

The inverse approach avoids biases caused by the Rayleigh wind speed distribution assumption (Wanninkhof et al. 2002). The more recent wind products have a higher fidelity and show significant deviation from a Rayleigh distribution on a regional and also global scale (Liu et al. 2008). Fig. 1 shows the wind speed distributions of the CCMP product and the NCEP-2 analysis (www.esrl.noaa.gov/psd/data/gridded/data.ncep.marine.html) and the corresponding Rayleigh distribution using the mean winds of these products. It is apparent that both the mean and distribution differ, which will impact the gas transfer velocity and gas fluxes, and yield different coefficients for the same constraints (Naegler et al. 2006). Several global gas flux products use the NCEP-2 analysis (Takahashi et al. 2009; Lana et al. 2011). The global mean wind speed for NCEP-2 of 7.6 m s⁻¹ is greater than the CCMP mean of 7.3 m s⁻¹. The distribution of NCEP-2 winds is broader than CCMP winds with a greater frequency of low winds (<4 m s⁻¹) and high winds (>15 m s⁻¹). The CCMP product has an appreciably higher frequency of winds in the intermediate range (4-12 m s⁻¹) and deviates from the Rayleigh distribution in that it is narrower and has a higher peak skewed toward the higher winds. It also shows a lower frequency of high winds. The differing wind speed distributions lead to a 0.2 Pg C y⁻¹ (≈15%) lower net CO_2 uptake by the ocean for the CCMP winds compared with the NCEP-2 winds, even after accounting for the differences in global mean wind by adjusting the coefficient "a" (Eq. 3). This is because low to intermediate winds are predominant sources of CO_2 to the atmosphere, and areas with high winds are predominantly sinks (Wanninkhof et al. 2009). The prevalence of intermediate winds in the CCMP wind product leads to a lower uncertainty in the fluxes, as the gas exchange-wind speed relationship is best constrained at intermediate winds.

The comparison between wind speed distribution of the global wind speed product and the corresponding Rayleigh distribution illustrates the inherent uncertainties in using

averaged products. The update of the gas exchange-wind speed relationship does not rely on a Rayleigh assumption. Equation 3 is expressed in terms of the mean of the wind speed squared or second moment, $<U^2>$, rather than the mean winds squared, $<U>^2$. Therefore, the relationship should be used with wind speed measurements of sufficiently short intervals to capture the full wind speed spectrum over the time interval of flux determination. A comparison of wind values obtained from buoys and ships measured at frequencies of 1 min or higher shows that for averaging times greater than a month the 6-h CCMP product at 0.25° spatial resolution used here captures the full variability spectrum.

CO_2 exchange is enhanced by hydration reactions with water or hydroxide ions at the interface (Hoover and Berkshire 1969; Emerson 1995; Wanninkhof and Knox 1996) that increases the CO_2 exchange at low winds. W-92 concluded that for global ocean applications the enhancement had little effect because of the infrequency of low winds and because gas exchange rate was small at low wind speeds over the ocean, even with chemical enhancement. In W-92, the chemical enhancement was modeled as an additive component. Subsequent studies and analyses suggest that this assumption leads to overestimates of the contribution of chemical reactions at the interface. Theoretical and laboratory studies show that the absolute impact of chemical enhancement decreases and becomes insignificant for winds greater than 6 m s^{-1}. Therefore, the updated relationship does not include chemical enhancement. The impact of this assumption is included in the uncertainty estimate.

The uncertainties in k for global CO_2 exchange is estimated based on literature values or estimates of the uncertainty in individual terms and a propagation of error in Eq. 4, assuming no cross-correlation between terms, as detailed in the discussion. The Schmidt number for CO_2 and its temperature dependence have an uncertainty of 5% (Jähne et al. 1987), and the coefficient "a" has a 10% uncertainty as estimated in Ho et al. (2011). The second moment of the winds in the 3-12 m s^{-1} wind speed range have an uncertainty of 4%, or 0.3 m s^{-1} at the global mean wind speed of 7.3 m s^{-1} (Hoffman et al. 2013). An ad hoc additive uncertainty in k of 10 % (0.3 cm h^{-1}) is included to account for the offset that results from chemical enhancement of k of 3 cm h^{-1} below U_{10} = 3.5 m s^{-1}. This estimate accounts for the fact that globally, winds below 3 m s^{-1} occur 16% of the time for the CCMP product (Fig. 1). Similarly an increased uncertainty of an additional 10% (17 [m s^{-1}]^2) for the second moment of the winds above 12 m s^{-1} that occur 10% of the time is included in the uncertainty estimate based on the increased uncertainty in the CCMP wind product at higher winds (Hoffman et al. 2013).

The cumulative error in k = 0.251 $<U^2>$ (Sc/660)$^{-0.5}$ is given by

$$\Delta k \ k^{-1} = 0.0251/0.251 + \Delta <U^2> / <U^2> + 0.5 \ \Delta Sc/Sc$$
$$+ \Delta \ k \ k^{-1}_{(k=3, U10<3.5)} + \Delta <U^2> / <U^2>_{U10>12} \qquad (9)$$

where $\Delta k \ k^{-1}$ is the fractional uncertainty in the gas transfer velocity. The last two terms are the uncertainties at low and high winds as described above. By including all terms, the uncertainty is

$$\Delta k \ k^{-1} = 0.1 + 0.04 + 0.025 + 0.01 + 0.02 = 0.20 \ \text{or} \ 20\% \qquad (10)$$

The additive fractional uncertainty estimate illustrates the impact of each term. The uncertainly in the coefficient accounts for half of the overall uncertainty followed by uncertainty in the winds. This conclusion is similar to that of Johnson (2010) who did not attempt to propagate the uncertainty but rather presented the individual terms.

Discussion

The relationship between gas exchange and wind speed, and the associated uncertainty is determined for CO_2 exchange over the ocean. Dedicated gas exchange studies over the ocean agree well with the proposed parameterization, but gas transfer in local environments could be different due to differing forcing and lead to different weighting of the factors influencing the uncertainty in k. The error analysis for global CO_2 exchange shows that the 10% uncertainty in the coefficient 0.251 that lumps all the complex interfacial processes controlling k into a single coefficient contributes most to the uncertainty. The assigned uncertainty of the coefficient is less than the 32% quoted in Sweeney et al. (2007) as the more recent uncertainty in the coefficient of Ho et al. (2011) is applied based on a compilation of field studies. The uncertainty analysis shows that the other factors influencing the uncertainty have a smaller but cumulative effect in that they double the overall uncertainty to 20%.

A rigorous uncertainty analysis of empirical gas transfer velocities for gas exchange-wind speed relationships is challenging in large part because of the poorly quantified assumptions of uncertainty of the individual components. For this reason, the cumulative uncertainty for k is seldom provided but rather the uncertainty of the most important components or the individual uncertainties of the components and the impact on k are provided (Johnson 2010). Here, the uncertainty in the gas transfer of CO_2 for global scale analyses is estimated from propagating the error for each term through Eq. 4 assuming no cross-correlation between terms. This allows for multiplicative error propagation rather than a mathematically complex Taylor expansion (Bevington and Robinson 1992). This uncertainty is for global scale estimates of CO_2 exchange using the second moment of the winds from the CCMP product. For uncertainties on regional or local scale analysis, or different wind products, the individual terms need to be adjusted for their respective uncertainty.

The error propagation through Eq. 4 assumes the coefficient 0.251, wind speed, and Schmidt number dependence are not cross-correlated. Whereas the magnitude of the coefficient and $<U^2>$ are closely related, their uncertainties are not neces-

sarily cross-correlated except at higher winds. The Schmidt number is a physical property that is not correlated with the wind or the coefficient but its dependency is a function of boundary layer turbulence (Jähne et al. 1984). The forcing of gas transfer changes at high winds by bubbles and at low winds by chemical enhancement, and the uncertainty is poorly constrained. Therefore an additive uncertainty is added for these regimes. The estimates for the uncertainty of the individual components are based uncertainties quoted in the literature and are not statistically rigorous in that the "uncertainty of the uncertainties" is undetermined. The uncertainty estimate in k is a simplified analysis applicable global scale k of CO_2 but a useful indicator of how the uncertainties in wind, coefficient, and Schmidt number impact k.

There are some caveats for use of the relationship for gases other than CO_2. Using the inverse square root Schmidt number dependence $(Sc/660)^{-0.5}$ is a valid means to apply the relationship for other gases at intermediate winds. However, for smooth surfaces at low winds, theory and measurements yield a $-2/3$ exponent for the Schmidt number dependence (Jähne et al. 1984). The impact of using a $-1/2$ dependence instead of a $-2/3$ dependence for low winds is small, as the range in Schmidt number for most gases is narrow, and the absolute value of gas transfer is low in this wind regime. Chemical enhancement will only be applicable for gases that react in the boundary layer. At high winds, the turbulence regime and gas specific exchange patterns due to bubbles lead to differing gas transfer velocities. However, the gas transfer in these regimes has been difficult to measure, describe, and model. Gases with lower solubility will be impacted by bubbles to a greater degree than gases with higher solubility. The separation between enhanced gas transfer due to bubbles and wave-induced turbulence at high winds has not been fully established and will be gas specific (Woolf 2005; Asher and Wanninkhof 1998). Field studies with dimethyl sulfide (DMS), which has a solubility of an order of magnitude greater than CO_2, show significantly lower gas transfer velocities at high winds than CO_2 (Yang et al. 2011; Bell et al. 2013). This suggests that bubble-mediated processes might have a large impact on gas transfer at high winds and cause large deviations for other gases compared with the relationship for CO_2 shown in Fig. 2. However, laboratory studies have not shown bubble effects of this magnitude (Asher et al. 1996). An alternative theory for the low exchange of DMS based on the surface activity of organic molecules on bubble surfaces has been proposed (Vlahos et al. 2011).

The molecular impacts on gas transfer are manifested through solubility and the Schmidt number. The solubility controls the concentration gradient between water and air. The coefficients in Table 2 are applicable to determine the solubilities at specified temperatures and salinities. Few updated solubility measurements are available, notably the solubility measurements for methyl bromide (De Bruyn and Saltzman 1997b) and radon (Schubert et al. 2012). The solubilities of a range of noble gases are currently being measured at the

Woods Hole Noble Gas Laboratory (R. Stanley pers. comm.).

The empirical relationships for the Schmidt number have been updated from those in W-92 to include relationships with temperature using measured diffusion coefficients for DMS, CFC11, CFC12, and SF_6 (King and Saltzman 1995; De Bruyn and Saltzman 1997a; Zheng et al. 1998) rather than estimate these coefficients from molecular characteristics using relationships proposed by Wilke and Chang (1955), as modified by Hayduk and Laudie (1974). The kinematic viscosity of seawater is determined from the dynamic viscosity and density as presented in Sharqawy et al. (2010). The Schmidt numbers are determined from -2 to 40°C and then fit to a fourth-order polynomial. As with the third-order polynomial relationships in W-92 that were for a temperature range from 0-30°C, the updated curve fits should not be used beyond the -2 to 40°C temperature range. Table 1 provides updated coefficients for the polynomial expression. Uncertainties in the polynomial expressions of Schmidt number with temperature are less than 5% and correspond to differences of 2.5% in the normalization factor $(Sc/660)^{-0.5}$.

Comments and recommendations

An updated coefficient for the gas exchange-wind speed relationship over the ocean is provided, along with a recommended global wind product that is available at high spatial and temporal resolution, alleviating the need for using averaged winds with their associated uncertainties. The relationship is based on similar overall principles and the methodology that was used in the W-92 relationship. The uncertainty in the relationship is 20%, which is based on a more comprehensive assessment than the uncertainty estimate of 25% for the relationship used in W-92 that was based solely on the estimated uncertainty in the bomb-^{14}C inventory. The smaller uncertainty is due to an improved understanding of the processes and a better quantification of global winds. It agrees well with field experiments using dual tracers. New estimates of the Schmidt number are provided, expanding the temperature range from -2 to 40°C.

The updated relationship is

$$k = 0.251 \langle U^2 \rangle \, (Sc/660)^{-0.5} \qquad (11)$$

The relationship is appropriate for regional-to-global flux estimates of CO_2 using the CCMP wind product at 6-hour and 0.25° resolution from which the second moment can be determined. It should provide good estimates for most insoluble gases at intermediate wind speed ranges (3-15 m s^{-1}). At low winds, non-wind effects such as chemical enhancement and thermal boundary layer processes influence gas transfer, and this quadratic relationship will underestimate gas transfer. At high winds ($\approx$> 15 m s^{-1}), bubble-enhanced exchange will affect gases differently depending on their solubility, and the relationship is only suitable for CO_2 under these conditions. The differences in physical and chemical processes in bound-

ary layers and their impact on gases at high and low winds need to be taken into consideration when estimating uncertainty. Since over 94% of the winds over the ocean are in the 3-15 m s^{-1} range, the regional and global gas transfer velocities for gases listed in Table 1 can be determined using the above relationship.

Acknowledgments

References

Asher, W., L. M. Karle, B. J. Higgins, and P. J. Farley. 1996. The influence of bubble plumes on air-seawater gas transfer velocities. J. Geophys. Res. 101:12027-10041 [doi:10.1029/96JC00121].

———, and R. Wanninkhof. 1998. Transient tracers and air-sea gas transfer. J. Geophys. Res. 103:15939-15958 [doi:10.1029/98JC00379].

Atlas, R., and others. 2011. A cross-calibrated multiplatform ocean surface wind velocity product for meteorological and oceanographic applications. Bull. Amer. Meteor. Soc. 92:157-174 [doi:10.1109/IGARSS.2008.4778804].

Bell, T. G., W. De Bruyn, S. D. Miller, B. Ward, K. Christensen, and E. S. Saltzman. 2013. Air/sea DMS gas transfer in the North Atlantic: evidence for limited interfacial gas exchange at high wind speed. Atmos. Chem. Phys. Discuss. 13:13285-13322 [doi:10.5194/acpd-13-13285-2013].

Bevington, P. R., and D. K. Robinson. 1992. Data reduction and error analysis for the physical sciences. McGraw-Hill.

Bullister, J. L., and D. P. Wisegarver. 1998. The solubility of carbon tetrachloride in water and seawater. Deep Sea Res. I 45:1285-1302 [doi:10.1016/S0967-0637(98)00017-X].

———, D. P. Wisegarver, and F. A. Menzia. 2002. The solubility of sulfur hexafluoride in water and seawater. Deep Sea Res. I 49:175-187 [doi:10.1016/S0967-0637(01)00051-6].

Broecker, W. S., T.-H. Peng, G. Östlund, and M. Stuiver. 1985. The distribution of bomb radiocarbon in the ocean. J. Geophys. Res. 99:6953-6970 [doi:10.1029/JC090iC04p06953].

———, and others. 1986. Isotopic versus micrometeorologic ocean CO_2 fluxes: A serious conflict. J. Geophys. Res. 91:10517-10527 [doi:10.1029/JC091iC09p10517].

Dacey, J. W. H., S. G. Wakeman, and B. L. Howes. 1984. Henry's law constants for dimethylsulfide in freshwater and seawater. Geophys. Res. Lett. 11:991-991 [doi:10.1029/GL011i010p00991].

De Bruyn, W. J., and E. S. Saltzman. 1997a. Diffusivity of methyl bromide in water. Mar. Chem. 57:55-59 [doi:10.1016/S0304-4203(96)00092-8].

———, and ———. 1997b. The solubility of methyl bromide in pure water, 35‰ sodium chloride and seawater. Mar. Chem. 56:51-57 [doi:10.1016/S0304-4203(96)00089-8].

Doney, S. C., and others. 2009. Mechanisms governing interannual variability in the upper ocean inorganic carbon system and air-sea CO_2 fluxes Deep Sea Res. II 56:640-655.

Emerson, S. 1995. Enhanced transport of carbon dioxide during gas exchange, p. 23-35. *In* B. Jähne and E. C. Monahan [eds.], Air-water gas transfer: selected papers from the third international symposium on air-water gas transfer. Aeon Verlag & Studio.

Erickson III, D. J. 1993. A stability-dependent theory for air-sea gas exchange. J. Geophys. Res. 98:8471-8488 [doi:10.1029/93JC00039].

Etcheto, J., and L. Merlivat. 1988. Satellite determination of the carbon dioxide exchange coefficient at the ocean-atmosphere interface: a first step. J. Geophys. Res. 93:15669-15678 [doi:10.1029/JC093iC12p15669].

Fairall, C. W., J. E. Hare, J. B. Edson, and W. McGillis. 2000. Parameterization and micrometeorological measurement of air-sea gas transfer. Boundary-Layer Meteor. 96:63-105 [doi:10.1023/A:1002662826020].

Glover, D. M., N. M. Frew, S. J. McCue, and E. J. Bock. 2002. A multi-year time series of global gas transfer velocity from the TOPEX/POSEIDON dual frequency normalized radar backscatter algorithm, p. 325-333. *In* M. Donelan, W. Drennan, E. Saltzman, and R. Wanninkhof [eds.], Gas transfer at water surfaces. AGU, Geophysical Monograph 127.

Graven, H. D., N. Gruber, R. Key, S. Khatiwala, and X. Giraud. 2012. Changing controls on oceanic radiocarbon: New insights on shallow-to-deep ocgravenean exchange and anthropogenic CO_2 uptake. J. Geophys. Res. 117:C10005 [doi:10.1029/2012JC008074].

Hayduk, W., and H. Laudie. 1974. Prediction of diffusion coefficients for non-electrolytes in dilute aqueous solutions. AIChE J. 20:611-615 [doi:10.1002/aic.690200329].

Ho, D. T., C. S. Law, M. J. Smith, P. Schlosser, M. Harvey, and P. Hill. 2006. Measurements of air-sea gas exchange at high wind speeds in the Southern Ocean: Implications for global parameterizations Geophys. Res. Let. 33:L16611 [doi:10.1029/2006GL026817].

———, R. Wanninkhof, P. Schlosser, D. S. Ullman, D. Hebert, and K. F. Sullivan. 2011. Toward a universal relationship between wind speed and gas exchange: Gas transfer veloci-

ties measured with ^{3}He/SF$_6$ during the Southern Ocean Gas Exchange Experiment. J. Geophys. Res. 116:C00F04 [doi:10.1029/2010JC006854].

Hoffman, R. N., J. V. Ardizzone, S. M. Leidner, D. K. Smith, and R. Atlas. 2013. Error estimates for ocean surface winds: applying Desroziers diagnostics to the cross-calibrated, multiplatform analysis of wind speed. J. Atmos. Ocean. Technol. 30:2596-2603 [doi:10.1175/JTECH-D-13-00018.1].

Hoover, T. E., and D. C. Berkshire. 1969. Effects of hydration in carbon dioxide exchange across an air-water interface. J. Geophys. Res. 74:456-464 [doi:10.1029/JB074i002p00456].

Jackson, D. L., G. A. Wick, and J. E. Hare. 2012. A comparison of satellite-derived carbon dioxide transfer velocities from a physically based model with GasEx cruise observations. J. Geophys. Res. 117:C00F13 [doi:10.1029/2011JC007329].

Jähne, B., W. Huber, A. Dutzi, T. Wais, and J. Ilmberger. 1984. Wind/Wave-tunnel experiment on the Schmidt number- and wave field dependence of air/water gas exchange, p. 303-309. *In* W. Brutsaert and G. H. Jirka [eds.], Gas transfer at water surfaces. Reidel.

———, G. Heinz, and W. Dietrich. 1987. Measurement of the diffusion coefficients of sparingly soluble gases in water with a modified Barrer method. J. Geophys. Res. 92:10767-10776 [doi:10.1029/JC092iC10p10767].

Johnson, M. T. 2010. A numerical scheme to calculate temperature and salinity dependent air-water transfer velocities for any gas. Ocean Sci. 6:913-932.

King, D. B., and E. S. Saltzman. 1995. Measurement of the diffusion coefficient of sulfur hexafluoride in water. J. Geophys. Res. 100:7083-7088 [doi:10.1029/94JC03313].

Krakauer, N. Y., J. T. Randerson, F. W. Primau, N. Gruber, and D. Menemenlis. 2006. Carbon isotope evidence for the latitudinal distribution and wind speed dependence of the air-sea gas transfer velocity. Tellus B 58:390-417.

Lana, A., and others. 2011. An updated climatology of surface dimethylsulfide concentrations and emission fluxes in the global ocean. Global Biogeochem. Cycles 25 [doi:10.1029/2010GB003850].

Liss, P. S. 1973. Processes of gas exchange across an air-water interface. Deep Sea Res. 20:221-238.

———, and L. Merlivat. 1986. Air-sea gas exchange rates: Introduction and synthesis, p. 113-129. *In* P. Buat-Menard [ed.], The role of air-sea exchange in geochemical cycling. Reidel.

Liu, W. T., W. Tang, and X. Xie. 2008. Wind power distribution over the ocean. Geophys. Res. Let. 35:L13808 [doi:10.1029/2008GL034172].

McGillis, W.R., J.B. Edson, J.E. Hare, and C.W. Fairall. 2001. Direct Covariance Air-Sea CO$_2$ Fluxes. J. Geophys. Res. 106, 16729-16745 [doi10.1029/2000JC000506].

———, and others. 2004. Air-sea CO$_2$ exchange in the equatorial Pacific. J. Geophys. Res. 109 [doi:10.1029/2003JC002256].

McNeil, C., and E. D'Asaro. 2007. Parameterization of air-sea gas fluxes at extreme wind speeds. J. Mar. Sys. 66:110-121 [doi:10.1016/j.jmarsys.2006.05.013].

Monahan, E. C., and M. C. Spillane. 1984. The role of oceanic whitecaps in air-sea gas exchange, p. 495-503. *In* W. Brutsaert and G. H. Jirka [eds.], Gas transfer at water surfaces. Reidel.

———, and H. G. Dam. 2001. Bubbles: an estimate of their role in the global oceanic flux of carbon. J. Geophys. Res. 106:9377-9383 [doi:10.1029/2000JC000295].

Naegler, T. 2009. Reconciliation of excess ^{14}C-constrained global CO$_2$ piston velocity estimates. Tellus B 61:372-384 [doi:10.1111/j.1600-0889.2008.00408.x].

———, P. Ciais, K. Rodgers, and I. Levin. 2006. Excess radiocarbon constraints on air-sea gas exchange and the uptake of CO$_2$ by the oceans. Geophys. Res. Lett. 33: L11802 [doi:10.1029/2005GL025408].

Nightingale, P. D., and others. 2000. In situ evaluation of air-sea gas exchange parameterizations using novel conservative and volatile tracers. Global Biogeochem. Cycles 14:373-387 [doi:10.1029/1999GB900091].

Peacock, S. 2004. Debate over the ocean bomb radiocarbon sink: closing the gap. Global Biogeochem. Cycl. 18:GB2022 [doi:10.1029/2003GB002211].

Risien, C. M., and D. B. Chelton. 2008. A global climatology of surface wind and wind stress fields from eight years of QuikSCAT scatterometer data. J. Phys. Oceanogr. 38:2379-2413 [doi:10.1175/2008JPO3881.1].

Rubin, S. I., and R. M. Key. 2002. Separating natural and bomb-produced radiocarbon in the ocean: The potential alkalinity method. Global Biogeochem. Cycl. 16:1105 [doi:10.1029/2001GB001432].

Saltzman, E. S., D. B. King, K. Holmen, and C. Leck. 1993. Experimental determination of the diffusion coefficient of dimethylsulfide in water. J. Geophys. Res. 98:16481-16486 [doi:10.1029/93JC01858].

Sasse, T. P., B. I. McNeil, and G. Abramowitz. 2013. A novel method for diagnosing seasonal to inter-annual surface ocean carbon dynamics from bottle data using neural networks. Biogeosciences 10:4319-4340 [doi:10.5194/bg-10-4319-2013].

Schubert, M., P. Albrecht, E. Lieberman, and W. Burnett. 2012. Air-water partitioning of ^{222}Rn and its dependence on water temperature and salinity. Energy Environ. Sci. 46:3905-3911.

Sharqawy, M. F., J. H. Lienhard, and S. M. Zubair. 2010. Thermophysical properties of seawater: a review of existing correlations and data. Desalin. Water Treatment 16:354-380 [doi:10.5004/dwt.2010.1079].

Smethie, W. M., T. T. Takahashi, D. W. Chipman, and J. R. Ledwell. 1985. Gas exchange and CO$_2$ flux in the tropical Atlantic Ocean determined from ^{222}Rn and pCO2 measurements. J. Geophys. Res. 90:7005-7022 [doi:10.1029/JC090iC04p07005].

Sweeney, C., and others. 2007. Constraining global air-sea gas exchange for CO$_2$ with recent bomb C-14 measurements.

Global Biogeochem. Cycles 21:GB2015 [doi:10.1029/2006GB002784].

Takahashi, T., and others. 2009. Climatological mean and decadal change in surface ocean pCO_2, and net sea-air CO_2 flux over the global oceans. Deep-Sea Res. II 2009:554-577 [doi:10.1016/j.dsr2.2008.12.009].

Telszewski, M., and others. 2009. Estimating the monthly pCO_2 distribution in the North Atlantic using a self-organizing neural network. Biogeosciences 6:1405-1421 [doi:10.5194/bg-6-1405-2009].

Vlahos, P., E. C. Monahan, B. J. Huebert, and J. B. Edson. 2011. Wind-dependence of DMS transfer velocity: comparison of model with recent southern ocean observations, p. 313-321. *In* S. Komori, W. McGillis, and R. Kurose [eds.], Gas transfer at water surfaces 2010. Kyoto Univ. Press.

Wallcraft, A. J., A. B. Kara, C. N. Barron, E. J. Metzger, R. L. Pauley, and M. A. Bourassa. 2009. Comparisons of monthly mean 10 m wind speeds from satellites and NWP products over the global ocean. J. Geophys. Res. 114:D16109 [doi:10.1029/2008JD011696].

Wanninkhof, R. 1992. Relationship between gas exchange and wind speed over the ocean. J. Geophys. Res. 97:7373-7381 [doi:10.1029/92JC00188].

———, and L. Bliven. 1991. Relationship between gas exchange, wind speed and radar backscatter in a large wind-wave tank. J. Geophys. Res. 96:2785-2796 [doi:10.1029/90JC02368].

———, and M. Knox. 1996. Chemical enhancement of CO_2 exchange in natural waters. Limnol. Oceanogr. 41:689-698 [doi:10.4319/lo.1996.41.4.0689].

———, S. C. Doney, T. Takahashi, and W. R. McGillis. 2002. The effect of using time-averaged winds on regional air-sea CO_2 fluxes, p. 351-357. *In* M. Donelan, W. Drennan, E. Saltzman, and R. Wanninkhof [eds.], Gas transfer at water surfaces. AGU, Geophysical Monograph 127.

———, W. E. Asher, D. T. Ho, C. S. Sweeney, and W. R. McGillis. 2009. Advances in quantifying air-sea gas exchange and environmental forcing. Ann. Rev. Mar. Science 1:213-244.

Warner, M. J., and R. F. Weiss. 1985. Solubilities of chlorofluorocarbons 11 and 12 in water and seawater. Deep Sea Res. 32:1485-1497 [doi:10.1016/0198-0149(85)90099-8].

Weiss, R. F. 1970a. Helium isotope effect in solution in water and seawater. Science 168:247-248 [doi:10.1126/science.168.3928.247].

———. 1970b. The solubility of nitrogen, oxygen and argon in water and seawater. Deep Sea Res. 17:721-735.

———. 1971. Solubility of helium and neon in water and sea-water. J. Chem. Eng. Data 16:235-241 [doi:10.1021/je60049a019].

———. 1974. Carbon dioxide in water and seawater: the solubility of a non-ideal gas. Mar. Chem. 2:203-215 [doi:10.1016/0304-4203(74)90015-2].

———, and T. K. Kyser. 1978. Solubility of krypton in water and seawater. J. Chem. Eng. Data 23:69-72 [doi:10.1021/je60076a014].

———, and B. A. Price. 1980. Nitrous oxide solubility in water and seawater. Mar. Chem. 8:347-359 [doi:10.1016/0304-4203(80)90024-9].

Wentz, F. J., S. Peteherych, and L. A. Thomas. 1984. A model function for ocean radar cross sections at 14.6 GHz. J. Geophys. Res. 89:3689-3704 [doi:10.1029/JC089iC03p03689].

Wiesenburg, D. A., and J. N. L. Guinasso. 1979. Equilibrium solubilities of methane, carbon monoxide, and hydrogen in water and sea water. J. Chem. Eng. Data 24:356-360 [doi:10.1021/je60083a006].

Wilhelm, E., R. Battino, and R. J. Wilcock. 1977. Low pressure solubility of gases in liquid water. Chem. Rev. 77:219-262 [doi:10.1021/cr60306a003].

Wilke, C. R., and P. Chang. 1955. Correlation of diffusion coefficients in dilute solutions. AIChE J. 1:264-270 [doi:10.1002/aic.690010222].

Wood, D., and R. Caputi. 1966. Solubilities of Kr and Xe in fresh and seawater. U.S. Naval Radiological Defense Laboratory.

Woolf, D. K. 2005. Parameterization of gas transfer velocities and sea-state-dependent wave breaking. Tellus B 57:87-94 [doi:10.1111/j.1600-0889.2005.00139.x].

Woolf, D. 2006. Recent developments in parameterization of air-sea gas exchange, p. 9-10. Flux news (WCRP).

Yang, M., B. W. Blomquist, C. W. Fairall, S. D. Archer, and B. J. Huebert. 2011. Air-sea exchange of dimethylsulfide in the Southern Ocean: Measurements from SO GasEx compared to temperate and tropical regions. J. Geophys. Res. 116:C00F05 [doi:10.1029/2010JC006526].

Zappa, C. J., and others. 2007. Environmental turbulent mixing controls on air-water gas exchange in marine and aquatic systems. Geophys. Res. Lett. 34 [doi:10.1029/2006GL028790].

Zheng, M., W. J. De Bruyn, and E. S. Saltzman. 1998. Measurements of the diffusion coefficients of CFC-11 and CFC-12 in pure water and seawater. J. Geophys. Res. 103:1375-1379 [doi:10.1029/97JC02761].